

Integrated trucks assignment and scheduling problem with mixed service mode docks: A Q-learning based adaptive large neighborhood search algorithm

Yueyi Li^a, Mehrdad Mohammadi^b, Xiaodong Zhang^{a,*}, Yunxing Lan^a, Willem van Jaarsveld^b

^aBeijing Jiaotong University, ShangYuanCun NO.3, Beijing, 100044, China

^bEindhoven University of Technology, PO Box 513, Eindhoven, 5600MB, Netherlands

Abstract

Mixed service mode docks enhance efficiency by flexibly handling both loading and unloading trucks in warehouses. However, existing research often predetermines the number and location of these docks prior to planning truck assignment and sequencing. This paper proposes a new model integrating dock mode decision, truck assignment, and scheduling, thus enabling adaptive dock mode arrangements. Specifically, we introduce a Q-learning-based adaptive large neighborhood search (Q-ALNS) algorithm to address the integrated problem. The algorithm adjusts dock modes via perturbation operators, while truck assignment and scheduling are solved using destroy and repair local search operators. Q-learning adaptively selects these operators based on their performance history and future gains, employing the epsilon-greedy strategy. Extensive experimental results and statistical analysis indicate that the Q-ALNS benefits from efficient operator combinations and its adaptive mechanism, consistently outperforming benchmark algorithms in terms of optimality gap and Pareto front discovery. In comparison to the predetermined service mode, our adaptive strategy results in lower average tardiness and makespan, highlighting its superior adaptability to varying demands.

Keywords: Assignment, Truck assignment and scheduling, Mixed service mode, Adaptive Large Neighborhood Search, Q-learning algorithm.

1. Introduction

Mixed Service Mode (MSM) is a flexible warehouse loading and unloading operation mode where a single dock can handle both inbound and outbound trucks. This is in contrast to the exclusive service mode, commonly seen in real-world terminals, where one side is designated for loading and the other for unloading. Boysen and Fließner (2010) introduced this term in their review, and several scholars (Stephan and Boysen 2011, Bodnar et al. 2017, Rijal et al. 2019) have conducted related research on this mode. Their results indicate that MSM docks can effectively reduce waiting time and operation costs. While most current studies focus on the cross-dock scenario, this study is driven by the operational needs of real-world unmanned warehouses and highlights the potential for broader applications in various warehouse operations. In fact, the MSM is increasingly gaining industry attention (Ladier and Alpan 2016). On the one hand, it addresses the need for intensive dock utilization; on the other hand, concerns about potential operational confusion can be alleviated by intelligent warehousing systems and equipment, which makes the mode more feasible.

When employing the MSM in warehouse operations, besides deciding *where and when* to schedule inbound and outbound trucks, another crucial decision is *how* to arrange the dock modes. In current

*Corresponding author: Xiaodong Zhang (zhangxd@bjtu.edu.cn)

research, the arrangement of MSM docks is often predetermined. Bodnar et al. (2017) pre-set the proportion of MSM docks among the total number of docks, and Rijal et al. (2019) pre-set the proportion and location of MSM docks. This study proposes a more flexible approach to the MSM, where the decision of each dock’s mode is part of the decision-making process. This means adapting the dock mode based on the structure of inbound and outbound trucks. Hereafter, the problem is referred to as the Integrated Trucks Assignment and Scheduling Problem with Dock Mode Decision (TASP-DMD).

The TASP-DMD problem is a typical NP-hard combinatorial optimization problem for which meta-heuristic algorithms can provide promising solutions. Literature has effectively solved related problems using the Adaptive Large Neighborhood Search (ALNS) meta-heuristic algorithm. Considering the convenient framework and proven success of ALNS, this paper also adopts this algorithm. In ALNS mechanisms, significant potential for improvement lies particularly in the Operator Filtering (OF) and Adaptive Operator Selection (AOS) (Pisinger and Ropke 2019). The OF process involves conducting comparative experiments to identify the most effective operators, thereby enhancing the overall performance. In ALNS, designing proper operators for specific problems is crucial (Windras Mara et al. 2022). While many operators have been proposed, there is little analysis of the appropriate number or effectiveness of these operators. Voigt (2024) tested and ranked operators in vehicle routing problems (VRP), showing that performance differences exist. Pre-set operators may perform well on similar instances but poorly on others with different characteristics. Thus, a thorough filtering of potential operators before their employment is necessary. The AOS process includes evaluating operator performance and selecting suitable ones for further exploration (Ropke and Pisinger 2006, Pisinger and Ropke 2007). This adaptiveness is achieved by continuously monitoring operator performance and adjusting the selection accordingly (Windras Mara et al. 2022), ensuring the search remains efficient and adaptive. Classical AOS mechanism follows the roulette wheel principle as Ropke and Pisinger (2006), while a few studied a stochastic universal sampling strategy (Chowdhury et al. 2019). However, according to Turkeš et al. (2021), the added value of simple methods for AOS is not significant, indicating that simple adaptive mechanisms might not be intelligent enough to focus on successful operators. Therefore, machine learning algorithms, which can rapidly capture environmental states and make decisions, have significant application potential in this area (Johnn et al. 2023, Boualamia et al. 2023). This paper combines Q-learning, as a reinforcement learning algorithm, with ALNS, attempting to leverage the model-free and learning-based advantage of Q-learning to improve AOS performance.

Motivated by research gaps and practice value, this paper seeks to address several research questions: 1) How can the TASP-DMD problem be modeled and solved effectively? 2) Will the decision to incorporate dock mode outperform the predetermined dock mode, and to what extent? 3) How to identify better-performing operator combinations within ALNS? and 4) Does the integration of Q-learning enhance the performance of ALNS, and to what extent?

For the existing research, the contributions of this paper are:

- We introduce new decision variables and constraints related to dock modes, integrating truck assignment, scheduling, and dock mode decisions. Comparative analysis with predetermined service modes demonstrates the model’s adaptability to various demands and optimized dock utilization.
- Filtering better-performing operators for ALNS. We adopt a pairwise comparison method to identify better-performing operator combinations from a wide range of local search and pertur-

bation operators. This OF process significantly improves the algorithm’s performance in solving the TASP-DMD problem by focusing on the most effective operators.

- Q-learning is embedded into the original ALNS framework to enhance the AOS process. By guiding decisions based on both historical operator performance and the current search state, the Q-Learning-based AOS mechanism makes more efficient choices. This results in superior performance when solving the TASP-DMD problem compared to benchmark algorithms, while maintaining comparable computational overhead.

The remainder of the paper is structured as follows. Section 2 presents an overview of existing research related to MSM docks scheduling, ALNS, and Q-learning. We formulate the problem in Section 3 and present our Q-ALNS in Section 4. Section 5 designs a set of experiments, and the computational results are reported in Section 6. This analysis leads to conclusions in Section 7.

2. Literature review

2.1. Truck assignment and scheduling for mixed service mode docks

Dock operational decisions focus on efficiently allocating limited dock resources to inbound and outbound trucks over a specific time period. Given the typical imbalance between the number of trucks and available docks, precise timing and sequencing are crucial to minimize waiting times for trucks on-site. From the comprehensive classification by Buijs et al. (2014) and Boysen and Flidner (2010), it is evident that the assignment and scheduling of trucks are critical operational decisions for docks. Previous research often equated dock scheduling with truck assignment and scheduling, as the number and configuration of docks are typically predetermined at the tactical level. However, with MSM docks, this equivalence no longer holds, as decisions on dock modes are required.

A comparative analysis of the most relevant literature on truck assignment and scheduling with MSM docks, as summarized in Table 1, highlights several key points. Most research focused on cross-docking, aiming for seamless transfers between inbound and outbound trucks with minimal storage buffers (Ladier and Alpan 2016). However, storage buffers are necessary for many other warehouse scenarios like distribution centers (DCs), and dock scheduling significantly influences internal resource management (Wolff et al. 2021). Only a few studies have considered internal resource constraints Wolff et al. (2021), Hermel et al. (2016). Research on the impact of MSM dock scheduling on internal operational processes is insufficient.

Existing studies on MSM docks (Stephan and Boysen 2011, Shakeri et al. 2012, Berghman and Leus 2015, Hermel et al. 2016) have not considered dock mode as a decision variable, often treating it as predetermined. Some studies, such as Bodnar et al. (2017) and Rijal et al. (2019), have recognized the benefits of MSM docks but treated the proportion of MSM docks as a fixed input. This approach limits the full flexibility of dock mode decisions and may lead to sub-optimal solutions.

Most related studies tend to employ heuristic-based algorithms. Recent research has begun using machine learning techniques to improve heuristic or exact algorithms. Neamatian Monemi and Gelareh (2023) used support vector machines to identify effective objective functions in different Benders decomposition stages, demonstrating the framework’s effectiveness. Combining RL and other machine learning techniques with heuristic-based algorithms requires further research. We aim to bridge these gaps by combining Q-learning, a model-free RL, with ALNS to improve solution efficiency and quality, specifically addressing TASP-DMD problems for DCs with MSM docks.

Table 1: Summary of the most related literature

Publications	Problem characteristic			Objective functions	Mode Variable	Algorithms
	Scenarios	MSM	Handling			
Shakeri et al. (2012)	C	Yes	Yes	makespan	No	two-phase HA
Berghman and Leus (2015)	DC	Yes	No	Tardiness, makespan	No	HA
Hermel et al. (2016)	C	Yes	Yes	Transshipment, makespan	No	Hierarchical HA
Bodnar et al. (2017)	C	Yes	No	Transshipment, tardiness	No	ALNS
Rijal et al. (2019)	C	Yes	No	Transshipment, tardiness, storage	No	ALNS
Wolff et al. (2021)	C	No	Yes	Internal resource requirements	No	CG + HA
Neamatian Monemi et al. (2023)	C	No	No	Transshipment	No	SVM+BD
This paper	DC	Yes	Yes	Tardiness, makespan, handling	Yes	Q-learning + ALNS

MSM: mixed service mode dock; C: cross-docking; HA: heuristic algorithm; DC: distribution center; CG: column generation; ALNS: adaptive large neighborhood search; SVM: support vector machine; BD: benders decomposition.

2.2. Original ALNS

ALNS is a meta-heuristic algorithm derived from the Large Neighborhood Search (LNS) introduced by Shaw (1998). ALNS enhances LNS by exploring large neighborhoods through multiple destroy and repair local search operators and an adaptive selection mechanism, enabling the convenient design of neighborhood structures based on decision content (Ropke and Pisinger 2006). A key element of ALNS is the careful design of appropriate operators, as well as the integration of an adaptive layer to dynamically select these operators during the search process (Windras Mara et al. 2022).

Rigorous analysis and test of operators (among multiple operators) are crucial to the success of ALNS (Karimi-Mamaghan 2022, Voigt 2024). The flexibility of the ALNS framework often leads researchers to include a large number of operators, increasing the chances of finding better solutions. However, an inappropriate set of operators can diminish algorithm efficiency. Scholars (Windras Mara et al. 2022, Turkeš et al. 2021) emphasized the importance of thorough operator analysis. In a related study, Voigt (2024) reviewed and ranked operators for the VRP problem and its variants, confirming variations in operator selection frequency. This paper underscores the necessity of evaluating and filtering operators tailored to specific problems. In the context of TASP-DMD problems, the abundance of operators requires careful filtering and selection based on their expected effectiveness.

In ALNS, the adaptive operator selection (AOS) mechanism typically selects operators based on their weights, which are often updated using a score-based method. In this method, operators are assigned scores based on their recent performance, which are then used to adjust their weights and influence their probability of being selected in the future. For example, Bodnar et al. (2017) assigned three types of scores to operators based on outcomes such as yielding a solution better than the global best, yielding a solution better than the current best, or no improvement. These scores are then used to update the weights of each operator accordingly. Similarly, Rijal et al. (2019) employed the same AOS mechanism for their study to handle dock allocation alongside truck scheduling. However, the score-based method often overlooked differences in operator performance, as it simply classified performance levels and was often user-defined (Johnn et al. 2023). Studies like Turkeš et al. (2021) have pointed out that the simple AOS mechanisms used in most ALNS offer limited improvement to the algorithm’s performance. Developing effective AOS mechanisms remains an open challenge. Learning-based methods like ML techniques have emerged as promising alternatives (Karimi-Mamaghan 2022). Johnn et al. (2023) introduced a deep RL-based operator selection mechanism for the capacitated VRP, demonstrating that this learning-based mechanism outperforms both random and score-based methods. Compared to score-based method, learning-based methods can capture richer information related to operator selection, leading to better overall performance.

2.3. Integration of Q-learning into ALNS

Q-learning is a widely used RL algorithm that enables agents to learn optimal policies through interactions with the environment. Its model-free nature makes it suitable for complex and dynamic settings where constructing an accurate model is challenging or infeasible. When integrated into ALNS, Q-learning can extract valuable insights from the search process and guide subsequent searches, leading to more adaptive and efficient outcomes. In Q-learning-based AOS, Q-value updates replace the traditional weight updates, where operators were previously assigned scores, and now they are assigned rewards (Johnn et al. 2023, Boualamia et al. 2023). Therefore, careful design of the reward scheme is crucial, as it determines the feedback each operator receives and directly influences the learning process. Zhang et al. (2022) used deep Q-learning to handle uncertainties in synchronized transportation planning, showing that RL-based operators outperform randomly implemented ones. Boualamia et al. (2023) incorporated Q-learning into the AOS mechanism of ALNS. Using the epsilon-greedy strategy, new operators are selected based on Q-value after reaching a local minimum. Computational results indicated that a Q-learning-based AOS mechanism enhances both the efficiency and average performance of the original ALNS. However, both studies focused on the VRP, and neither tested the effectiveness of reward mechanisms. In a related field, Karimi-Mamaghan et al. (2023) combined Q-learning with the iteration greedy algorithm. They proposed a value-based AOS mechanism, which differs from the score-based method by directly updating Q-values based on the amount of improvement an operator achieves. Their approach demonstrates improvements in both solution quality and convergence rate, serving as an important inspiration for this work.

3. Problem description and formulation

3.1. Problem description

We consider an unmanned distribution center (UDC) that needs to allocate a set of trucks, T , including inbound I and outbound O trucks. Inbound trucks $i \in I$ can be assigned to either the unloading-only or mixed-mode docks. Outbound trucks $j \in O$ can be allocated to either the loading-only or mixed-mode docks. As depicted in Figure 1, the UDC is equipped with several dock doors D . Each dock $k \in D$ can operate in one of the three modes: loading-only (k_l), unloading-only (k_u), or mixed-mode (k_m).

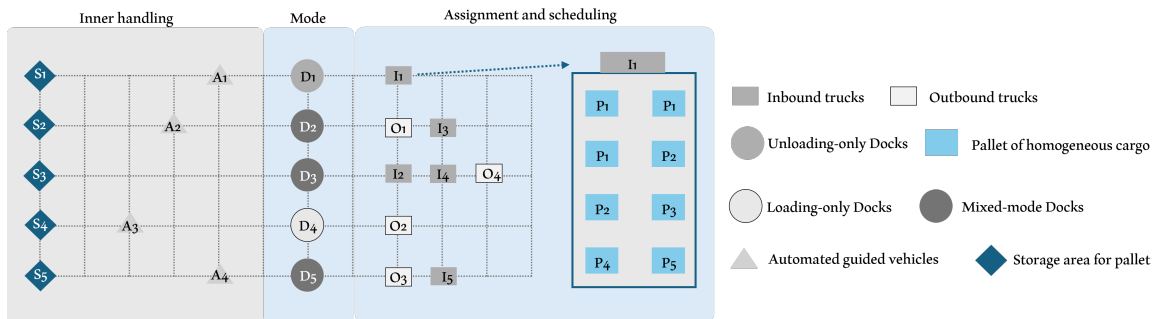


Figure 1: Truck assignment and scheduling problem with mixed-mode dock

Trucks' arrivals are scheduled in advance and have fixed arrival and expected departure times, denoted by time windows (r_i, d_i) . The lower bound of the time window cannot be moved earlier, but the upper bound can be extended, as departure times may extend beyond scheduled windows due to resource constraints. All cargo is palletized on standard-sized pallets, with each pallet containing

homogeneous cargo, denoted as P . The types and quantities of pallets $p \in P$ for inbound trucks are known, as are the types and quantities of pallets that need to be loaded onto outbound trucks. The UDC has a storage area S where the storage location $s \in S$ of each pallet u_{ps} is known. Based on the design capacity of the UDC, we assume that storage space constraints will not be exceeded. Inbound trucks, once assigned to a dock, need to unload pallets, which are then handled in the corresponding storage area by Automated Guided Vehicles (AGVs). Conversely, for outbound trucks, AGVs handle pallets from the storage area to the assigned dock for loading onto the trucks. Most research does not consider the impact of internal cargo transport, focusing more on the completion time of tasks at the truck end. However, in resource-limited situations, the efficiency of internal transport is a crucial factor for overall warehouse efficiency (Wolff et al. 2021). Therefore, including AGV transport distance as an objective quantifies the impact of each decision on the efficiency of the entire inbound and outbound process and controls the scheduling process with a focus on both transportation and warehouse system needs. Additionally, due to the switch between loading and unloading tasks, MSM docks require a reaction time τ before a task begins.

The scheduling decisions encompass the mode of the dock, truck-to-dock assignment, and truck scheduling, collectively termed the Integrated Truck Assignment and Scheduling Problem with Dock Mode Decision (TASP-DMD). The optimization objectives include minimizing truck delay, the maximum completion time, and the weighted distance of cargo handling. The truck delay accounts for any extensions beyond the scheduled departure time d_i , while the weighted distance of cargo handling considers the distance between the dock and the storage area.

Several assumptions have been made in this paper based on practical cases and experience: 1) Each dock is designed to be equipped with sufficient forklifts, and the travel paths of the forklifts are fixed, simplifying loading and unloading time to the time per pallet, denoted as t_e ; 2) Trucks can only begin operations after their scheduled arrival time; 3) A truck can leave the docking position only after completing its loading or unloading tasks; 4) No ad-hoc truck loading or unloading tasks are included; and 5) Compatibility between docking positions and truck types is not considered.

3.2. Notations

Before proposing the mathematical model of the problem, parameters and decision variables are listed in Table 2.

3.3. Truck assignment and scheduling model with dock mode decision

This section constructs a multi-objective mixed-integer programming model that simultaneously optimizes dock mode, truck assignment, and truck scheduling. The optimization objectives are to minimize dock operation delay time (referred to as tardiness), the maximum completion time (referred to as makespan), and the distance of cargo handling (referred to as distance).

Table 2: Notation Definitions for TASP-DMD Problem

Symbol	Notation Definition
Parameters	
r_i	Scheduled arrival time of truck i , $\forall i \in T$.
d_i	Expected departure time of truck i , $\forall i \in T$.
t_e	Loading and unloading time per unit of cargo.

Continued on next page

Table 2 – continued from previous page

Symbol	Notation Definition
τ	Additional waiting time required before each truck starts loading and unloading operations at mixed-mode docks.
a_i	Start time of operations for truck i , $\forall i \in T$.
e_i	End time of operations for truck i , $\forall i \in T$.
h_{ip}	Number of pallets of cargo type p to be unloaded or loaded on truck i , $\forall p \in P$, $\forall i \in T$.
A_i	Total quantity of cargo to be unloaded or loaded on truck i , $A_i = \sum_{p \in P} h_{ip}$.
v	Travel speed of the handling equipment provided at each dock.
u_{ps}	is 1 when cargo of type p are stored in area s , and is 0 otherwise.
N_D	Number of docks.
H_i	Total time for truck i 's loading or unloading tasks
H_{max}	Number of docks.
Decision Variables	
x_{ik}	is 1 if truck i designated for unloading is assigned to operate at dock k , and is 0 otherwise
y_{jk}	is 1 if truck j designated for loading is assigned to operate at dock k , and is 0 otherwise
λ_k	is 1 if dock k is exclusively for unloading, and is 0 otherwise
ρ_k	is 1 if dock k is exclusively for loading, and is 0 otherwise
μ_k	is 1 if dock k is for mixed-mode, and is 0 otherwise
z_{ijk}	is 1 if truck i and truck j are assigned to dock k , and i is the preceding truck in the sequence before j , and is 0 otherwise
Auxiliary Variables	
f_{ik}	is 1 if truck i is first in the sequence at dock k , and is 0 otherwise
l_{ik}	is 1 if truck i is last in the sequence at dock k , and is 0 otherwise

The tardiness refers to the sum of the delays of all trucks' operations compared to their scheduled departure times. The expression for the first objective function is shown in eq. (1). Here, δ_i represents the delay time for truck i , defined as $\delta_i = \max\{0, e_i - d_i\}$, where e_i is the time when truck i finishes its operations.

$$f_1 = \min \sum_{i \in I \cup O} \delta_i \quad (1)$$

The makespan refers to the latest time by which all loading and unloading tasks are completed. The expression for the second objective function is presented in eq. (2).

$$f_2 = \min \max\{e_i \mid i \in I \cup O\} \quad (2)$$

Assigning trucks to different docking positions results in varying distances for internal handling. The third objective function aims to minimize the total distance for handling. The expression for this objective function is detailed in eq. (3). Detailing the scheduling of AGVs would significantly increase the complexity of the problem. Therefore, we adopt the Euclidean distance between dock positions and storage locations. The distance m_{ks} between dock position k and storage location s is given by eq. (4), where Δx_{ks} and Δy_{ks} are the horizontal and vertical distances between them, respectively. Detailed scheduling will be addressed in future research.

$$f_3 = \min \sum_{i \in I, j \in O} \sum_{k \in D} \sum_{s \in S} \sum_{p \in P} x_{ik} h_{ip} u_{ps} m_{ks} \quad (3)$$

$$m_{ks} = \sqrt{(\Delta x_{ks})^2 + (\Delta y_{ks})^2} \quad (4)$$

The first category of constraints pertains to the allocation of dock positions. Eq. (5) ensures that each dock is designated for only one service type: unloading-only (λ_k), loading-only (ρ_k), or mixed-mode (μ_k). Eq. (6) and eq. (7) specify that each truck is assigned to only one dock. Eq. (8) ensures that unloading trucks are assigned only to docks that are capable of handling unloading, specifically exclusive unloading docks or MSM docks. Eq. (9) applies a similar logic to outbound trucks.

$$\lambda_k + \mu_k + \rho_k = 1, \forall k \in D \quad (5)$$

$$\sum_{k \in D} x_{ik} = 1, \forall i \in I \quad (6)$$

$$\sum_{k \in D} y_{jk} = 1, \forall j \in O \quad (7)$$

$$\sum_{k \in D} (\lambda_k x_{ik} + \mu_k x_{ik}) = 1, \forall i \in I \quad (8)$$

$$\sum_{k \in D} (\rho_k y_{jk} + \mu_k y_{jk}) = 1, \forall j \in O \quad (9)$$

The second category of constraints deals with the timing of truck loading and unloading operations. Eq. (10) defines the sequential relationship in time for trucks serviced at each docking position, with H_i representing the time for inbound and outbound operations. The value is determined as in eq. (13). Here, the first term accounts for the forklift's loading and unloading time, the second term for AGV handling time, and the third term for the preparation time required at mixed-mode docks. The sum includes all these times only when both μ_k and x_{ik} are set to 1. Eq. (11) and eq. (12) represent the time window constraints.

$$a_i + H_i \leq a_j + M(1 - z_{ijk}), \forall i, j \in I \cup O, k \in D \quad (10)$$

$$a_i + H_i \leq H_{\max}, \forall i \in I \cup O \quad (11)$$

$$a_i \geq r_i, \forall i \in I \cup O \quad (12)$$

$$H_i = \frac{A_i}{t_e} + \sum_{g \in G} \sum_{s \in S} \sum_{k \in D} x_{ik} h_{ip} u_{ps} m_{ks} \cdot \frac{1}{v} + \sum_{k \in D} \mu_k x_{ik} \tau \quad (13)$$

The third category of constraints pertains to the sequencing or ordering of trucks. Eq. (14) addresses the potential confusion in the assignment of truck sequencing variables, stipulating that if truck i precedes truck j at the same dock, then j cannot precede i at that dock. Eq. (15) indicates that z_{ijk} can only be 1 if trucks i and j are assigned to the same dock. Eq. (16) ensures that trucks i (unloading) and j (loading) are assigned to the same dock only when $\mu_k = 1$, providing a linear representation of the constraint $x_{ik} y_{jk} \leq \mu_k$. Eq. (17) to eq. (20) define the constraints for when a truck's loading or unloading sequence is either first or last at a dock, utilizing auxiliary variables f_{ik} and l_{ik} , which are set to 1 when a truck is the first or last in sequence at dock k , and 0 otherwise.

$$z_{ijk} + z_{jik} \leq 1, \forall i, j \in I \cup O, k \in D \quad (14)$$

$$z_{ijk} \leq x_{ik} x_{jk}, \forall i, j \in I \cup O, k \in D \quad (15)$$

$$x_{ik} + y_{jk} - 1 \leq \mu_k, \forall i \in I, j \in O, k \in D \quad (16)$$

$$f_{ik} + \sum_{j \in I \cup O \setminus i} z_{jik} = x_{ik}, \forall i \in I \cup O, k \in D \quad (17)$$

$$l_{ik} + \sum_{j \in I \cup O \setminus i} z_{ijk} = x_{ik}, \forall i \in I \cup O, k \in D \quad (18)$$

$$\sum_{i \in I \cup O} f_{ik} = 1, \forall k \in D \quad (19)$$

$$\sum_{i \in I \cup O} l_{ik} = 1, \forall k \in D \quad (20)$$

The final category of constraints pertains to the types of variables.

$$x_{ik}, y_{jk} \in \{0, 1\}, \forall i \in I, j \in O, k \in D \quad (21)$$

$$\lambda_k, \mu_k, \rho_k \in \{0, 1\}, \forall k \in D \quad (22)$$

$$z_{ijk} \in \{0, 1\}, \forall i, j \in I \cup O, k \in D \quad (23)$$

$$f_{ik}, l_{ik} \in \{0, 1\}, \forall i \in I \cup O, k \in D \quad (24)$$

$$a_i \geq 0, \forall i \in I \cup O \quad (25)$$

The model, implemented in Python 3.8 and utilizing the Gurobi 11.0.1, was evaluated to demonstrate its practicality and accuracy. The test data includes six docks and twenty trucks, where eight trucks are for unloading and twelve are for loading. The model was tested on a computer with an Intel[®] Core(TM) i7-10210U processor, 1.6GHz, 4GB memory, running Windows 11, using the Visual Studio platform. The solution process took 1.23 seconds, yielding optimal values $f_1 = 0$, $f_2 = 105.06$, and $f_3 = 3818.5$. The results are presented in Table 3.

Table 3: Optimal solution for a small-scale example

Dock	Mode	Truck order	Dock	Mode	Truck order
D_1	Unloading-only	1 → 6	D_4	Loading-only	13 → 15 → 17 → 12 → 10
D_2	Unloading-only	7 → 2	D_5	Loading-only	16 → 9 → 11 → 20
D_3	Mixed-mode	3 → 5 → 8 → 4	D_6	Loading-only	14 → 18 → 19

4. Proposed ALNS with a Q-learning-based AOS: Q-ALNS

Figure 2 illustrates the flowchart of the proposed Q-ALNS. Additionally, Algorithm 1 provides the detailed Pseudo-code of the Q-ALNS. The main improvements of the proposed Q-ALNS over the original ALNS are as follows:

1) The main loop is extended into a two-layer loop. The outer loop employs perturbation operators to achieve diverse neighborhood searches for dock mode decisions. The inner loop uses destroy and repair local search operators for truck assignment and scheduling under the new dock mode. This approach allows for the simultaneous optimization of dock mode, truck assignment, and scheduling.

2) The Q-learning algorithm is integrated into the AOS mechanism, which bases its decisions on the search state and history of performance. The gray areas in Figure 2 illustrate this mechanism. During the local search phase of the algorithm, each combination of destroy and repair operators forms an action. After applying an action, a corresponding reward is immediately obtained based on the improvement in the solution quality. Then, the Q-learning algorithm assigns a credit to this action and updates the Q-table. Unlike score-based methods, Q-learning also accounts for future gains, encouraging long-term benefits. The next action is selected using the ϵ -greedy strategy. This strategy uses the Q-table to choose actions with the highest credit or explore new actions, preventing the algorithm from getting stuck in local optima.

3) Since we are dealing with a multi-objective model, our algorithm updates solutions by maintaining and updating a Pareto set of solutions. A new solution is accepted under one of the following four conditions: when the new Pareto solution dominates the current global best solution, the global best solution is updated; when the new Pareto solution dominates the current local best solution, the local best solution is updated; when the new solution and the current global best solution are mutually non-dominating, the new solution is added to the Pareto set; and when the new solution does not meet any of the above criteria, it is accepted according to the Metropolis acceptance function Karimi-Mamaghan et al. (2023).

4.1. States and actions in the proposed Q-ALNS

In the proposed Q-ALNS, Q-learning is utilized to select local search operators at each iteration, as illustrated in Algorithm 2. The set of actions is correspondingly defined to determine which local search operator to apply, represented as eq. (26), where a is the number of operators. Each operator is associated with a set of destroy

Algorithm 1: Pseudo-code for ALNS with Q-learning (Q-ALNS)

```
Input:  $p$  // Perturbation operators
Input:  $op$  // Local search operators
Input:  $A$  // Action space
Input:  $\epsilon \in \mathbb{R}$  // Epsilon-greedy parameter
Input:  $\beta \in \mathbb{R}$  // Epsilon-decay
Input:  $\alpha \in \mathbb{R}$  // Learning rate
Input:  $\gamma \in \mathbb{R}$  // Discount factor
Input:  $E \in \mathbb{N}$  // Size of iteration
Input:  $L \in \mathbb{N}$  // Size of learning loop
Input:  $\eta \in \mathbb{R}$  // Global improvement weight
Input:  $t \in \mathbb{N}$  // Increment non_improve counter
Output:  $\chi^*$  // Optimized solution found

1 Function ALNS( $\epsilon, \beta, \alpha, \gamma, E, \eta, A, t$ ):
2    $\chi \leftarrow \text{initialsolution}()$  // Construct initial solution
3    $\chi^* \leftarrow \chi$  // Initialize best solution
4    $Q \leftarrow [0]$  // Initialize Q-table
5    $s \leftarrow 0$  // Initialize state
6    $a \leftarrow \text{randomchoice}(A)$  // Initialize action
   // Outer loop
7   for  $e \leftarrow 1$  to  $E$  do
8      $R_{\text{prev}} \leftarrow R_{\min}(\chi)$  // Remember current local optimum before a local search episode
9      $R_{\text{prev}}^* \leftarrow R_{\min}(\chi^*)$  // Remember the best solution found before a local search episode
10     $R \leftarrow R_{\text{prev}}$  // Remember the best local optimum found during an episode
11     $R^* \leftarrow R_{\text{prev}}^*$  // Remember the best solution found during an episode
12    if  $e < L$  then
13       $a \leftarrow \text{randomchoice}(A)$  // Action is drawn randomly from A
14    else
15       $a \leftarrow \text{Q-learning}(R_{\text{prev}}, R_{\text{prev}}^*, R, R^*, \epsilon, \beta, \alpha, \gamma, E, \eta, A, s, op)$  // Action based on Q-table
   // Inner loop
16    $\text{non\_improve} \leftarrow 0$  // Initialize non_improve counter
17    $T \leftarrow -\sum f_k(\text{sol}) / \log(0.5)$  // Initialize temperature
18   while  $\text{non\_improve} < t$  do
   // destroy and repair phase
19    $\chi' \leftarrow N(\chi, op)$  // local search episode
   // Update best solution found
20   if Pareto dominate( $\chi', \chi^*$ ) then
21      $\chi^* \leftarrow \chi'$ 
22      $R^* \leftarrow R_{\min}(\chi^*)$ 
23   else if Pareto dominate( $\chi', \chi$ ) then
24      $\chi \leftarrow \chi'$ 
25      $R \leftarrow R_{\min}(\chi)$ 
26   else if mutually non-dominating( $\chi', \chi^*$ ) then
27      $\chi'$  to Pareto set
28   else if accept( $\chi', \text{temperature criterion}$ ) then
29      $\chi \leftarrow \chi'$ 
30      $\text{non\_improve} \leftarrow \text{non\_improve} + 1$ 
31   else
32      $\text{non\_improve} \leftarrow \text{non\_improve} + 1$ 
33    $\text{update } T$  // Update temperature
34    $\text{update } Q, s$  // Update q-table
35    $\chi \leftarrow P(\chi^*, p)$  // Do perturbation
36 return  $\chi^*$  // Return the best solution
```

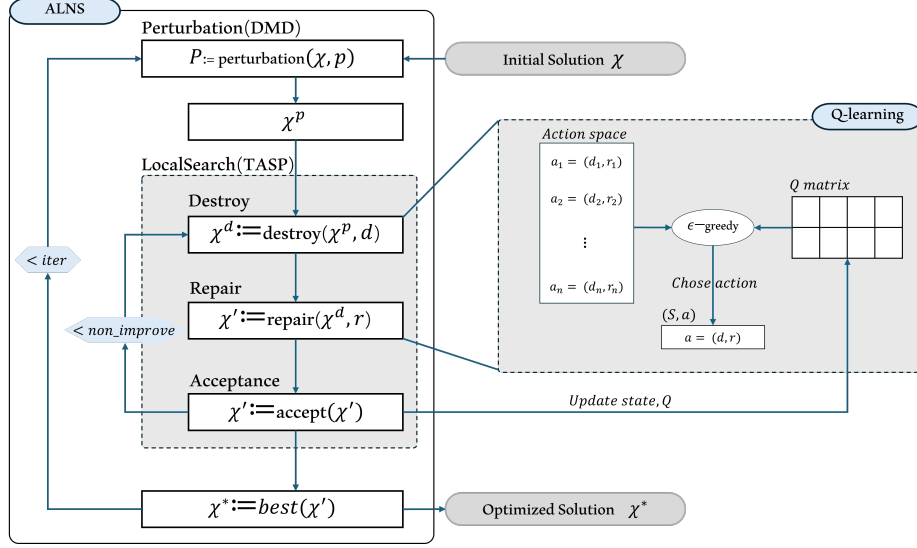


Figure 2: Flowchart of the Q-ANLS

and repair operations. Upon selecting an action, the corresponding operations are performed on the current solution χ , leading to a new solution χ' .

Algorithm 2: Pseudo-code for Q-learning Function

Input: $R_{prev}, R_{prev}^*, R, R^*, \epsilon, \beta, \alpha, \gamma, E, \eta, A, s, op$
Output: Q, s', a' // New state s' and next action a'

- 1 **Function** $Q\text{-learning}(R_{prev}, R_{prev}^*, R, R^*, \epsilon, \beta, \alpha, \gamma, E, \eta, A, s, op)$:
 - // Calculate reward based on equations
 - 2 $r \leftarrow \text{CalculateReward}(R_{prev}, R_{prev}^*, R, R^*, e, \eta)$
 - // Determine state based on improvement during the iteration
 - 3 **if** $R^* < R_{prev}^*$ **then**
 - 4 $s' \leftarrow 1$
 - 5 **else**
 - 6 $s' \leftarrow 0$
 - // Update Q-table
 - 7 $Q(s, a) \leftarrow Q(s, a) + \alpha(r + \gamma \max_{a'} Q(s', a') - Q(s, a))$
 - // Apply epsilon-decay strategy to move from exploration to exploitation gradually
 - 8 $\epsilon \leftarrow \epsilon \cdot \beta$
 - // Choose an action using ϵ -greedy strategy
 - 9 **if** $\text{rand}() \geq \epsilon$ **then**
 - 10 $a' \leftarrow \text{argmax}_{a''} Q(s', a'')$
 - 11 **else**
 - 12 $a' \leftarrow \text{randomchoice}(A)$
 - 13 **return** Q, s', a'

$$A = \{1, 2, \dots, a\} \quad (26)$$

In Q-learning, a state represents the condition or situation of the environment at a particular time. It is a critical factor in deciding the action to be taken to achieve the optimal solution. The state is determined by evaluating whether the current solution shows any improvement, thus indicating whether the algorithm is trapped in a local optimum. Therefore, in the Q-learning mechanism of this study, the state is set as a binary set $S = \{0, 1\}$. If new state $s' = 0$, it implies that the local search in the latest iteration could not find a better solution. Conversely, if $s' = 1$, it means that a better solution was found after the latest iteration. Let Δ denotes the improvement measure, the state transition function $P(s' | s, a)$ based on this rule is then as follows:

$$P(s' | s, a) = \begin{cases} 1 & \text{if } \Delta > 0 \text{ and } s' = 1 \\ 1 & \text{if } \Delta \leq 0 \text{ and } s' = 0 \\ 0 & \text{otherwise} \end{cases} \quad (27)$$

In each iteration of the Q-ANLS, the performance of the local search operators is evaluated, and the reward is calculated accordingly. The Q-table is then updated based on this reward and the current s , as eq. (28). Finally, using the ϵ -greedy strategy, the next local search operator is selected based on the current state and the updated Q-table.

$$Q(s, a) = Q(s, a) + \alpha \left(r + \gamma \max_{a'} Q(s', a') - Q(s, a) \right) \quad (28)$$

4.2. Reward function in the proposed Q-ALNS

The reward in Q-learning represents the feedback received after taking an action, reflecting the benefit of that action in improving the current solution. In each iteration of the Q-ALNS, a local search operator is selected, and a local search is performed until no further improvement is achieved. Thus, the evaluation of the performance of a local search operator is conducted at the end of each iteration. The reward can be defined in various ways. In this work, we reference the definition proposed by Karimi-Mamaghan et al. (2023) to avoid the algorithm getting stuck in local optima and accelerate convergence. In their work, the reward is a function of global and local improvements of the solutions. Building on their methods, we incorporate the consideration of iteration count to assign higher values to greater improvements at later iterations, as illustrated in Algorithm 3.

The improvement in the solution includes enhancements in both global and local optima, computed using eq. (29) and eq. (30), respectively. These improvements are combined linearly in eq. (31), and multiplied by the iteration count to calculate the reward r (see eq. (32)), where e is the iteration count and C is a normalization constant. Due to the difference in magnitude between iteration counts and improvement values, the result is normalized by dividing by a constant. A penalty mechanism was also incorporated: if no improvement is obtained, the reward is adjusted to include the opportunity cost OC, reflecting the maximum prior improvement of unselected local search operators, as described in eq. (33).

$$\Delta\text{Global} = \max \left(\frac{R^* - R_{prev}^*}{R_{prev}^*}, 0 \right) \quad (29)$$

$$\Delta\text{Local} = \max \left(\frac{R - R_{prev}}{R_{prev}}, 0 \right) \quad (30)$$

$$\Delta\text{Improvement} = \Delta\text{Global} \times \eta + \Delta\text{Local} \times (1 - \eta) \quad (31)$$

$$r_1 = \frac{\Delta\text{Improvement} \times e}{C} \quad (32)$$

$$r_2 = \frac{(\Delta\text{Improvement} - \text{OC}) \times e}{C} \quad (33)$$

5. Experimental design

5.1. Experimental setting

The study scenario in this research is based on an unmanned warehouse X , located in Linyi City, Shandong Province, China. This warehouse primarily serves to consolidate and store regional less-than-truckload (LTL) cargo. Efficient warehouse operations, especially during inbound and outbound processes, are critical. Warehouse X features docks on both sides for loading and unloading. Storage positions within the warehouse are allocated based on proximity to these docks, with the goal of storing goods as close as possible to the loading and unloading areas. Although Warehouse X has an I-shaped layout, its operational flow more closely resembles a U-shape, making it well-suited for using MSM docks (Rijal et al. 2019). In this layout and service mode, the

Algorithm 3: Q-learning Reward Calculation with Penalty Mechanism

```

Input:  $R^*$ ,  $R_{prev}^*$ ,  $R$ ,  $R_{prev}$ ,  $\eta$ ,  $e$ ,  $C$ 
Output:  $r$  // Reward
1 Function CalculateReward( $R^*$ ,  $R_{prev}^*$ ,  $R$ ,  $R_{prev}$ ,  $e$ ,  $\eta$ ):
   // Calculate Global and Local Improvements
2    $\Delta_{Global} \leftarrow \max\left(\frac{R^* - R_{prev}^*}{R_{prev}^*}, 0\right)$ 
3    $\Delta_{Local} \leftarrow \max\left(\frac{R - R_{prev}}{R_{prev}}, 0\right)$ 
   // Calculate Weighted Improvement
4    $\Delta_{Improvement} \leftarrow \Delta_{Global} \cdot \eta + \Delta_{Local} \cdot (1 - \eta)$ 
5    $OC \leftarrow \max(\Delta_{Improvement})$ 
   // Check for Improvement
6   if  $\Delta_{Global} > 0$  or  $\Delta_{Local} > 0$  then
7      $r \leftarrow \frac{\Delta_{Improvement} \times e}{C}$ 
8   else
9      $r \leftarrow \frac{(\Delta_{Improvement} - OC) \times e}{C}$  // Include opportunity cost if no improvement
10  return  $r$ 

```

docks at both ends are not designated exclusively for unloading or loading; their functions are determined based on the demand structure, which aligns well with on-site management needs.

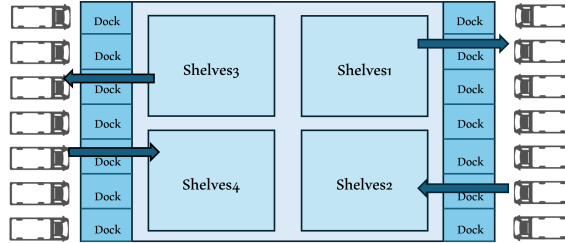


Figure 3: Layout and typical operational flow of warehouse X

To verify the effectiveness of the proposed algorithm, we apply it to a real-world scenario involving seven docks, using truck arrival and departure data along with cargo types collected from surveys. By adjusting the scale of docks and trucks, we form ten sets of test instances, as shown in Table 4. Each truck has a predefined type, arrival and expected departure time window, total cargo volume, and the quantity of each cargo type. The positions of the docks and shelves are represented by coordinates, with the corresponding shelf number for each cargo type known. Following this setup, we design a three-phase experiment.

Table 4: Set of test instances for TASP-DMD

Instance	Number of Docks	Number of Trucks	Instance	Number of Docks	Number of Trucks
1	3	20	6	8	100
2	4	30	7	8	130
3	5	50	8	9	160
4	6	60	9	9	180
5	7	70	10	10	200

In Phase 1, we conduct the operator filtering (OF) experiments to identify better-performing operator combinations. The goal is to pinpoint the operators that exhibit superior performance. In the Q-ALNS, the outer loop consists of several perturbation operators, and the inner loop includes a set of local search operators. Given our two-layer loop structure, the experiment is designed to first compare the performance of local search operators, addressing the question, “Which local search operators perform better?” After this, we combine the better-performing local search operators with perturbation operators to determine “Which perturbation operators perform better?”

In Phase 2, we use a set of benchmarks to validate and evaluate the competitiveness of the proposed Q-ALNS, as outlined in Table 5. $ALNS.i$ refers to the original ALNS, with i indicating different combinations of operators

based on the number of better-performing operators identified. RLNS replaces the AOS mechanism in the ALNS framework with a random selection mechanism. S-ALNS is a commonly used score-based ALNS in literature (Bodnar et al. 2017, Rijal et al. 2019). Gurobi 11.0.1 is also included as a commercial solver for comparison. The evaluation comprehensively covers multiple aspects: efficiency and accuracy through comparison with benchmarks, multi-objective optimization capabilities via analysis of Pareto fronts, and adaptability to various problem instances. We also examine the impact of different parameter settings, action set size, and reward functions on the algorithm’s performance. These analyses ensure a thorough understanding of the strengths of the Q-ALNS.

Table 5: Comparison benchmarks against the Q-ALNS

Index	Benchmark algorithm	Comparison purpose
1	ALNS _i	Effectiveness of multiple operator combinations against a single operator combination
2	RLNS	
3	S-ALNS	Effectiveness of Q-learning-based AOS
4	Gurobi	Validate and Evaluate multi-objective optimization capabilities

In Phase 3, we analyze different dock mode strategies to demonstrate the effectiveness of the improvements in our model. Previous studies have explored several common dock operation strategies, including exclusive mode (fixed loading and unloading dock assignments), partial mix mode (pre-setting some MSM docks), and fully mixed mode (pre-setting all docks as MSM docks). To achieve greater flexibility, this paper introduces an adaptive dock mode decision strategy. To validate the effectiveness of this strategy, we compare it with the exclusive mode and the fully mixed mode. Since the partial mix mode closely resembles the strategy proposed in this paper, it is excluded from the comparison. We refer to the three strategies compared as Adaptive (this paper), Fix, and Mix strategies.

5.2. Performance comparison metrics

Each experiment, involving various instances, operators, and mechanisms, was independently run 10 times. For each run, we recorded the mean, the best value found for every objective, and CPU time. The comparison metrics used in the experiment are shown in Table 6.

Table 6: Comparison Metrics used in the experiments

Phase	Metric	Index	Purpose
1	Dominate ratio	Z_i	Quality
2	Relative percentage deviation	RPD	Accuracy
2	Time taken to reach the best solution	CPU time	Efficiency
2	Nondominance Ratio	NR	Quality
2	Hypervolume	HV	Diversity
2	Hierarchical cluster counting	HCC	Uniformity
3	Relative percentage deviation	RPD	Accuracy
3	Time taken to reach the best solution	CPU time	Efficiency

In Phase 1, we used a dominance ratio metric to quantify the performance advantage of each local search and perturbation operator in our experiments. The dominance ratio Z_i for a given operator op_i is defined as the proportion of pairwise comparisons where op_i shows a statistically significant performance improvement over other operators. The result of this test is denoted as $\zeta_{i,j}$, where:

$$\zeta_{i,j} = \begin{cases} 1 & \text{if } op_i \text{ significantly outperforms } op_j, \\ -1 & \text{if } op_i \text{ is significantly outperformed by } op_j, \\ 0 & \text{if there is no significant difference between } op_i \text{ and } op_j. \end{cases} \quad (34)$$

Next, we use eq. (35) to count the number of times each operator op_i wins in the comparison. Here, n represents the total number of operators, and $\delta(\cdot)$ is the indicator function, which equals 1 if the condition inside is true and 0 otherwise. The dominance ratio Z_i is then calculated as the ratio of the count C_i to the total number of pairwise comparisons, using eq. (36).

$$C_i = \sum_{j=1, j \neq i}^n \delta(\zeta_{i,j} = 1) \quad (35)$$

$$Z_i = \frac{C_i}{n} \quad (36)$$

In Phase 2, we evaluate the quality of the solutions using two types of methods. We first focus on three key metrics: relative percentage deviation (RPD) of the mean and best values, and the average computational time (CPU time) required to obtain the best solution. Lower values in these metrics indicate better performance of operators and selection mechanisms. As the tardiness objective is a shared concern for both trucks and warehouses, the RPD calculation is based on the tardiness. The formula for RPD is provided in eq. (37), where R_i represents the tardiness value of experiment i , and R_{best} is the best objective value (tardiness) found among all experiments.

$$\text{RPD}_i = \frac{(R_i - R_{\text{best}})}{R_{\text{best}}} \times 100\% \quad (37)$$

To evaluate the ability to find Pareto fronts, we employ three metrics: nondomination ratio (NR) (Tan et al. 2001), hypervolume (HV) (Zitzler and Thiele 1999), and hierarchical cluster counting (HCC) (Guimaraes et al. 2009). The NR measures the proportion of solutions in the combined Pareto front that are non-dominated. Let P_B and P_C be the Pareto solution sets obtained by two different algorithms B and C , respectively. The NR is calculated as eq. (38), where $|\cdot|$ denotes the cardinality of the set. A higher NR value indicates that algorithm B contributes more useful candidate solutions to the combined Pareto front, reflecting its superior performance.

$$\text{NR}_B = \frac{|\{\mathbf{x} \in P_B \mid \mathbf{x} \text{ is nondominated in } P_{B \cup C}\}|}{|P_{B \cup C}|} \quad (38)$$

The formula for HV is provided in eq. (39), where S represents the set of Pareto solutions, (f_1, \dots, f_m) are the objective functions, and (f_1^*, \dots, f_m^*) is the reference point. This metric calculates the volume of the objective space that is dominated by the Pareto front and bounded by the reference point. It provides a measure of both the convergence and diversity of the solutions.

$$\text{HV}(S) = \text{volume} \left(\bigcup_{x \in S} [f_1(x), f_1^*] \times \dots \times [f_m(x), f_m^*] \right) \quad (39)$$

The HCC metric assesses the diversity of solutions by performing hierarchical clustering and counting the resulting clusters. The process involves applying a clustering algorithm to group the solutions and then summing the distances between these clusters. The formula for HCC is provided in eq. (40), where k represents the number of clusters and d_i denotes the distances between them. This metric offers insights into the distribution and variety of solutions within the Pareto front.

$$\text{HCC} = \sum_{i=1}^{k-1} d_i \quad (40)$$

In Phase 3, we continue to use RPD and CPU time as metrics for comparison. Furthermore, all statistical comparisons are conducted using the Wilcoxon signed-rank test (Wilcoxon 1992). This step is essential to ensure the stability and reliability of the results across different instances and run times, enabling us to validate whether the observed differences in performance are statistically significant. This analysis confirms the robustness of the proposed algorithm across various scenarios.

5.3. Parameters tuning

Our algorithm includes eight key parameters: τ , ϵ , β , α , γ , t , η , and l , as shown in Table 7. For parameter tuning, we employ response surface methodology (RSM). We begin by applying the Box-Behnken design method to create 112 parameter combinations. These combinations were tested on 10 instances, each run 5 times, with a stopping criterion of 400 outer loops. This criterion was based on the convergence trends observed in our experiments, which indicated that approximately 400 generations represent the overall trend. We then determine

the optimal parameter combination using RSM and Pareto optimization. A detailed analysis of each parameter’s influence on performance is provided in Section 6.

Table 7: Parameters of the Q-ALNS, their corresponding levels, and tuned values

Parameter	Notation	Levels			Tuned value
		-1	0	1	
Temperature scale	τ	0.01	0.105	0.2	0.2
Epsilon-greedy	ϵ	0.7	0.85	1	1
Epsilon-decay	β	0.99	0.995	1	0.99
Learning rate	α	0.5	0.75	1	0.5
Discount factor	γ	0.7	0.85	1	0.7
Non_improve times	t	10	25	40	20
Local/global improvement weight	η	0.6	0.7	0.8	0.8
Learning loop	l	100	200	300	200

6. Numerical and statistical results

This section executes the three-phase experiment outlined in Section 5 to validate the effectiveness and competitiveness of the Q-ALNS. All experiments were conducted using Python 3.8 on the Snellius Cluster High-Performance Computer, specifically on an AMD Rome 7H12 with CPUs running at 2.6 GHz with 32GB of RAM. Unless otherwise stated, the comparison results have passed significance tests.

6.1. Phase 1: Comparison between operators

In this phase, we identify the most advantageous operators for the problem through a series of experiments, assessing their impact on search quality and efficiency.

Common ranking methods in the literature for comparing operator performance include frequency-based, ablation-based, and pairwise comparison matrices. Given the multiple operators in the Q-ALNS, we employ the pairwise comparison metric method using the Wilcoxon test. This approach involves comparing operators in pairs and filling a pairwise comparison matrix based on statistically significant performance differences, resulting in a dominance matrix for all operators.

The local search operators in the Q-ALNS consist of destroy and repair operators, as listed in Table 8. These operators are selectively combined into specific combinations, each tailored to the objective functions (see Table 9). The sources and detailed descriptions are provided in Appendix A. For the perturbation phase of the algorithm, we design three types of perturbation operators tailored for unloading-only (I), loading-only (O), and mixed-mode (F) docks, as shown in Table 10.

Table 8: Description of local search operators

ID	Index	Destroy or repair operation
1	rRd	Randomly remove a truck from all available trucks
2	rMxTar	Remove the truck causing the most significant delay
3	rMxM	Remove the truck with the greatest weighted cargo handling distance
4	iBck	Swap the removed truck with its preceding truck at the same dock
5	iFwd	Swap the removed truck with its succeeding truck at the same dock
6	iSwap	Swap the removed truck with another randomly selected unloading or loading truck
7	iUp	Reallocate the removed truck to a dock with a higher rank based on handling distance
8	iDown	Reallocate the removed truck to a dock with a lower rank based on handling distance
9	iDockInsert	Insert the removed truck at all positions in the truck sequence of the same dock
10	iBtwInsert	Insert the removed truck randomly in the truck sequence of different docks
11	riInD2D	Swap trucks between two unloading docks
12	riOuD2D	Swap trucks between two loading docks
13	riFlxD2D	Swap trucks between two mixed-mode docks

Table 9: The combination of local search operators used in the Q-ALNS

ID	Operators	Target	ID	Operators	Target
op_1	rRd & iBck	Sequence Adjustment	op_9	rMxM & iUp	Sequence & Dock Adjustment
op_2	rRd & iFwd	Sequence Adjustment	op_{10}	rRd & iDockInsert	Sequence & Dock Adjustment
op_3	rRd & iSwap	Sequence & Dock Adjustment	op_{11}	rRd & iBtwInsert	Sequence & Dock Adjustment
op_4	rRd & iUp	Dock Adjustment	op_{12}	rMxTar & iDockInsert	Sequence & Dock Adjustment
op_5	rRd & iDown	Dock Adjustment	op_{13}	rMxTar & iBtwInsert	Sequence & Dock Adjustment
op_6	rMxTar & iBck	Sequence Adjustment	op_{14}	riInD2D	Dock Adjustment
op_7	rMxTar & iSwap	Distance & Dock Adjustment	op_{15}	riOuD2D	Dock Adjustment
op_8	rMxM & iSwap	Distance & Dock Adjustment	op_{16}	riFlxD2D	Dock Adjustment

Table 10: Description of perturbation operators

ID	Index	Perturbation operation
P_1	Chn2I	Randomly selects a dock and changes its type to unloading-only (I)
P_2	Chn2F	Randomly selects a dock and changes its type to mixed-mode (F)
P_3	Chn2O	Randomly selects a dock and changes its type to loading-only (O)

In the OF experiments, we evaluate the performance of local search operators in the inner loop. Each local search operator op_i is independently tested over 10 instances with 100 iterations each, and each experiment is repeated 10 times to ensure reliability. We set a dominance ratio threshold of 40% to identify better-performing local search operators. Operators that outperform 40% of others in pairwise comparisons are considered superior. With three prioritized objective functions $f_1 > f_2 > f_3$, operators are filtered accordingly. The filtering process, illustrated in Figure 4, identify operators op_2 , op_9 , and op_{11} as the better-performing local search operators. Additionally, we compare the performance of perturbation operators in the outer loop over 30 iterations and find that P_1 significantly outperforms P_0 and P_2 .

From the OF experiments, we reduce the original set of 16 local search operators to 3 and identify a single effective perturbation operator. Figure 5 shows the performance comparison among three sets of operators: all operators (ALL), all perturbation operators combined with the three better-performing local search operators ('3P+3op'), and the better-performing perturbation operator combined with the three better-performing local search operators ('P+3op'). The 'P+3op' set achieves better values across all objective functions and demonstrates higher stability, with a moderate increase in CPU time.

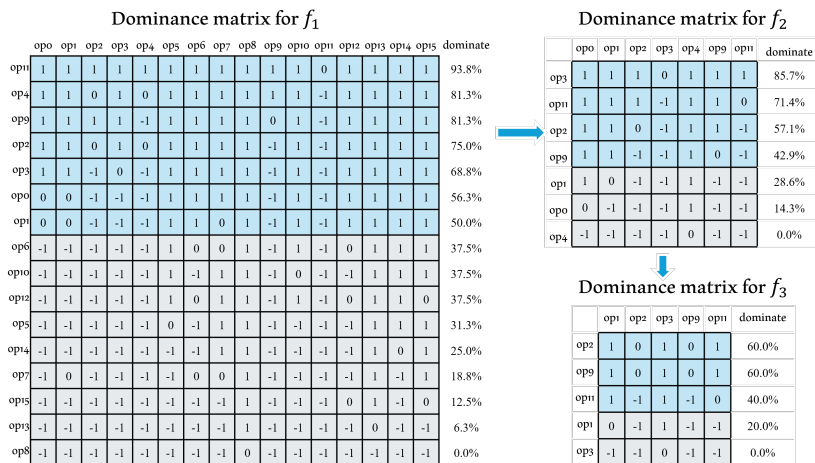


Figure 4: Local search operator filtering based on the Wilcoxon dominance matrix

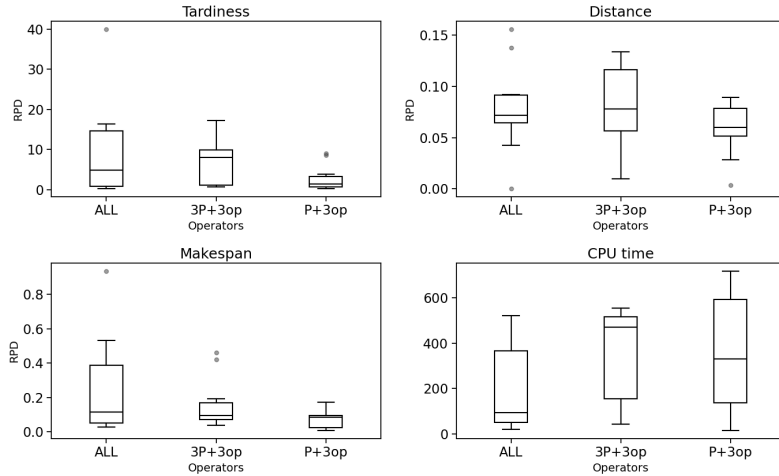


Figure 5: Comparison of three types of operators sets for the instance with 7 docks and 70 trucks

6.2. Phase 2: Performance analysis of the Q-ALNS against benchmark algorithms

In this stage of the experiment, we first compare three ALNS- i mechanisms with RLNS to assess the impact of better-performing operator combinations on the exploration-exploitation capability of the ALNS. Next, we compare the Q-ALNS with RLNS and the commonly used S-ALNS to demonstrate the effectiveness of the Q-learning-based operator selection mechanism compared to random and score-based selection mechanisms.

6.2.1. Comparison based on optimality gap and CPU time

Table 11 presents the performance of three ALNS- i algorithms, RLNS, S-ALNS, and the Q-ALNS, across 10 instances. Since we filtered three local search operators, the ALNS- i algorithm has three versions: ALNS_1, ALNS_2, and ALNS_3. The “AvS” column shows the average RPD (ARPD) of each algorithm from 10 independent runs per instance, while the “BS” column displays the RPD of the best solution. The “T(s)” column indicates the average CPU time. Figure 6a shows the boxplots of RPD for tardiness and CPU time, respectively.

Comparison of ALNS_1, ALNS_2, ALNS_3, and RLNS data shows RLNS performs better in both “AvS” and “BS” (lower values). Figure 6a shows RLNS with a lower mean (red dots) and minimum value, and a smaller interquartile range, indicating better robustness. This indicates that the use of multiple operators, as seen in RLNS, significantly enhances the competitiveness of ALNS in solving the TASP-DMD problem, compared to relying on individual operators. While all algorithms utilize the best operators, RLNS benefits from combining multiple operators, leading to improved performance.

The Q-ALNS achieves better AvS and BS values across all instances, particularly excelling in large-scale cases. It consistently performs well across different instance scales. The “Average” row in Table 11 indicates that Q-learning improves ARPD and best RPD by 9.0% and 52.9%, respectively, compared to RLNS, and by 9.4% and 49.8% compared to S-ALNS. According to the average CPU time reported in Table 11 and the CPU time boxplot in Figure 6a, the additional mechanisms of Q-ALNS introduce some overhead complexity. The Q-ALNS initially shows the longest CPU time, especially for smaller instances. However, as instance sizes increase, the relative CPU time for it decreases, and it is no longer the highest. This change reflects better scalability and efficiency in larger problem sizes.

We further compared the convergence behavior of the algorithms. Figure 6b shows the convergence curves of all algorithms for the representative cases (3_20 and 10_200). The Q-ALNS demonstrates a lower convergence curve with consistent behavior during the search process. It shows faster initial convergence, as evidenced by the rapid decline in its convergence curve during early iterations, and achieves lower final convergence values, reflecting its capability to find better final solutions. The convergence curves of Q-ALNS are smoother and exhibit less fluctuation, suggesting a more stable search process and reduced interference from local optima.

Table 11: Overall comparison of the Q-ALNS and classical ALNS

Instance set		ALNS_1			ALNS_2			ALNS_3			RLNS			S-ALNS			Q-ALNS		
Dock	Truck	AvS	BS	T(s)	AvS	BS	T(s)	AvS	BS	T(s)	AvS	BS	T(s)	AvS	BS	T(s)	AvS	BS	T(s)
3	20	2.749	2.618	4.2	1.939	1.875	24.6	0.624	0.320	43.8	0.290	0.155	25.3	0.258	0.151	25.8	0.256	0.008	28.7
4	30	0.479	0.419	6.0	0.629	0.629	41.6	0.461	0.413	49.4	0.183	0.113	49.6	0.163	0.097	49.4	0.179	0.080	40.4
5	50	0.344	0.273	9.7	0.509	0.473	82.4	0.337	0.226	108.0	0.085	0.029	108.8	0.076	0.004	108.0	0.065	0.023	118.9
6	60	0.087	0.042	11.6	0.232	0.221	99.4	0.221	0.151	132.3	0.094	0.028	135.0	0.095	0.059	132.3	0.075	0.029	154.1
7	70	8.795	8.622	13.6	9.322	9.095	133.2	1.015	0.576	560.9	0.386	0.218	247.6	0.446	0.198	254.5	0.367	0.106	216.4
8	100	0.196	0.180	19.8	0.308	0.302	231.8	0.086	0.060	940.9	0.030	0.016	424.0	0.028	0.013	440.7	0.030	0.012	412.2
8	130	0.057	0.045	26.3	0.144	0.135	363.0	0.062	0.049	1585.7	0.029	0.020	700.1	0.028	0.016	712.3	0.030	0.016	702.2
9	160	0.063	0.055	32.7	0.141	0.138	498.5	0.031	0.024	2652.2	0.015	0.007	1149.4	0.019	0.011	1135.2	0.015	0.003	1128.4
9	180	0.046	0.035	37.1	0.140	0.134	628.7	0.038	0.023	3418.4	0.021	0.014	1471.5	0.024	0.016	1545.9	0.015	0.006	1404.4
10	200	0.041	0.037	42.8	0.140	0.137	707.9	0.027	0.020	5253.6	0.018	0.012	2172.7	0.018	0.009	2289.8	0.014	0.006	1973.5
Average		1.286	1.233	20.374	1.350	1.314	281.097	0.290	0.186	1505.232	0.115	0.061	648.402	0.115	0.057	669.385	0.105	0.029	617.6

19

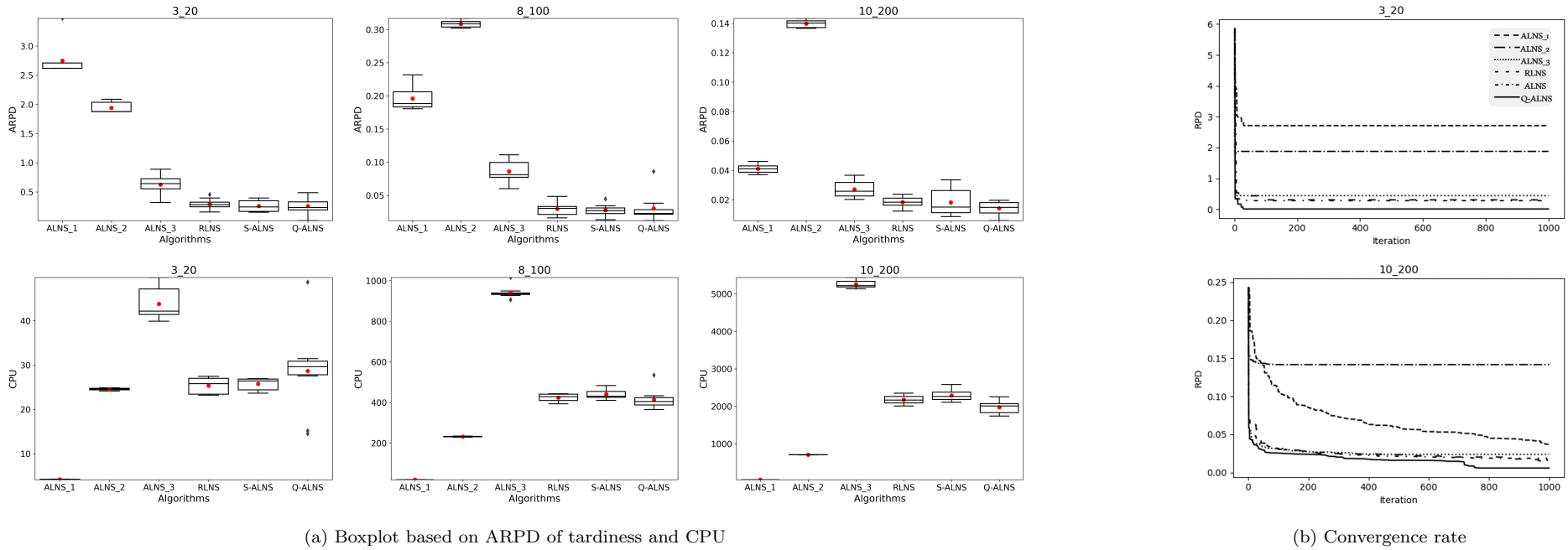


Figure 6: Comparison of the Q-ALNS, RLNS, S-ALNS, and ALNS_i based on different metrics

This phase of experiments demonstrates the successful identification of better-performing operators suitable for the TASP-DMD problem. The integration of the Q-learning mechanism significantly enhances the algorithm’s exploration of the solution space. While the Q-ALNS initially requires more computational time for smaller instances, its performance improves with larger problem sizes. This trade-off is justified by the significant improvements in solution quality and algorithm stability. These findings confirm that the Q-learning-based AOS mechanism not only improves solution quality but also ensures a more robust and efficient search process.

6.2.2. Comparison based on Pareto front

This section compares the Q-ALNS with Gurobi and RLNS to demonstrate its ability to find Pareto fronts. Gurobi solutions, obtained using the ϵ -constrains method, where f_2 and f_3 are relaxed into constraints and solved with Gurobi 11.0.1 and Python 3.8, result in an approximate Pareto front.

Due to time constraints, Gurobi failed to find optimal solutions for most instances, so three small-scale instances were designed for comparison. Based on the data in Table 12, the Q-ALNS shows superior performance compared to Gurobi. It achieves a higher proportion of non-dominated solutions (NR) on average (51.9%) compared to Gurobi (48.1%), demonstrating better quality in finding Pareto-optimal solutions. It also outperforms Gurobi in hypervolume (HV), with an average HV of 0.638 compared to Gurobi’s 0.577, indicating a more comprehensive exploration of the solution space. Expectedly, Gurobi performs better in hierarchical cluster counting (HCC), with an average HCC of 3.507 compared to Q-ALNS’s 2.380, indicating better solution uniformity. Overall, the Q-ALNS is comparable to or better than Gurobi, validating its effectiveness in solving the TASP-DMD problem.

For larger-scale instances, the Q-ALNS is compared with RLNS, as shown in Table 13. The Q-ALNS demonstrates superior performance over RLNS in most instances. It achieves a higher average NR value (0.653) compared to RLNS (0.347), indicating greater effectiveness in producing non-dominated solutions. In terms of HV, it averages 0.732, slightly outperforming RLNS’s 0.668, although the p -value of 0.375 indicates no significant difference. For HCC, the Q-ALNS performs better, with an average HCC of 15.011 compared to RLNS’s 8.524, suggesting more evenly distributed solutions.

6.2.3. Adaptiveness of the Q-ALNS to problem instances

This section analyzes how the Q-ALNS adaptively selects local search operators based on problem characteristics. We use the relative improvement index (RI) (Karimi-Mamaghan et al. 2023) to evaluate the contribution of different local search operators throughout the search process. RI is calculated by eq. (41), where $R(a)$ represents the average improvement per application of local search operator a over the entire search process. $R(a)$ is determined by eq. (42), where $GI(a)$ represents the total global improvement contributed by operator a and $S(a)$ represents the number of improvements achieved by operator a . $RI(a)$ then expresses this average improvement as a percentage of the total improvement achieved by all local search operators.

$$RI(a) = \frac{R(a)}{\sum_{a' \in A} R(a')} \times 100\% \quad (41)$$

$$R(a) = \frac{GI(a)}{S(a)} \quad (42)$$

Figure 7 shows the RI results for three randomly selected instances with varying characteristics, including dock-to-truck ratios and problem sizes ranging from small to large. The pie charts illustrate the distribution of the RI for three different local search operators ($a = 1, a = 2, a = 3$) across the three instances (4_30, 7_70, and 9_160). The results show clear variations in each operator’s contribution depending on the instance characteristics. For example, in instance 4_30, operator $a = 3$ has the highest contribution at 61.3%, while in instance 7_70, operator $a = 2$ dominates with 69.5%. As problem size increases, such as in instances 9_160, operator $a = 3$ becomes increasingly dominant, contributing over 83%. These results demonstrate the Q-ALNS’s ability to adaptively select the most suitable local search operators according to problem features, efficiently handling a wide range of problem scales and complexities.

Figure 8 provides a detailed visualization of operator selection throughout the search process for typical instances 4_30 and 10_200. Different colored bars represent the selected local search operator for each iteration (red for $a = 1$, purple for $a = 2$, and green for $a = 3$), while the black solid line represents the convergence curve. The charts show the dynamic selection of local search operators during the search process. In instance 4_30, the algorithm predominantly uses operator $a = 1$ (red), contributing significantly to rapid convergence. In instance 10_200, as the problem size increases, operator $a = 3$ (green) becomes crucial in the mid to late iteration. This dynamic adaptation of operator selection throughout the iterations underscores the Q-ALNS’s ability to tailor its search strategy based on evolving problem characteristics, enhancing search efficiency and improving solution quality across different problem scales.

Table 12: Overall comparison of the Q-ALNS with Gurobi based on Pareto front

Instance		NR		HV		HCC	
Dock	Truck	Gurobi	Q-ALNS	Gurobi	Q-ALNS	Gurobi	Q-ALNS
6	20	30.0%	70.0%	0.313	0.310	3.588	2.096
7	20	50.0%	50.0%	0.721	0.768	3.254	2.535
8	20	64.3%	35.7%	0.698	0.835	3.679	2.509
Average		48.1%	51.9%	0.577	0.638	3.507	2.380

Table 13: Overall comparison of the Q-ALNS with RLNS based on Pareto front

Instance		NR		HV		HCC	
Dock	Truck	RLNS	Q-ALNS	RLNS	Q-ALNS	RLNS	Q-ALNS
3	20	0.648	0.352	0.775	0.827	5.670	8.363
4	30	0.434	0.566	0.779	0.758	9.437	15.611
5	50	0.269	0.731	0.502	0.709	7.743	14.079
6	60	0.430	0.570	0.769	0.585	8.198	17.983
7	70	0.484	0.516	0.915	0.775	9.280	23.192
8	100	0.384	0.616	0.833	0.692	13.165	20.849
8	130	0.308	0.692	0.734	0.682	6.937	14.113
9	160	0.206	0.794	0.575	0.815	8.394	10.377
9	180	0.111	0.889	0.458	0.712	7.301	12.064
10	200	0.275	0.725	0.507	0.785	9.893	14.415
Average		0.347	0.653	0.668	0.732	8.524	15.011

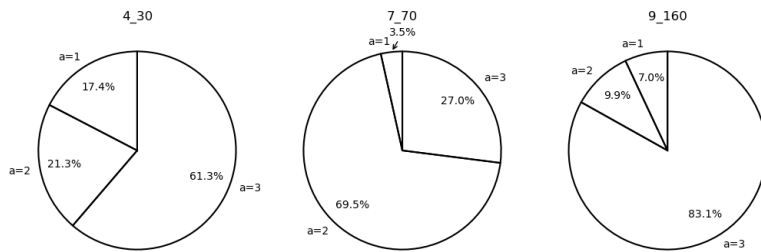


Figure 7: Average improvement performance of each local search operator in certain instances

6.2.4. Sensitivity analysis

This section conducts a sensitivity analysis of the Q-ALNS’s parameters, action space, and reward mechanism to assess how variations in these components affect the algorithm’s performance and robustness.

Q-ALNS parameters

The sensitivity analysis focuses on the impact of parameters on tardiness, distance, and makespan. The correlation heatmap (Figure 9) reveals that ϵ and t have significant negative effects on all objectives, making

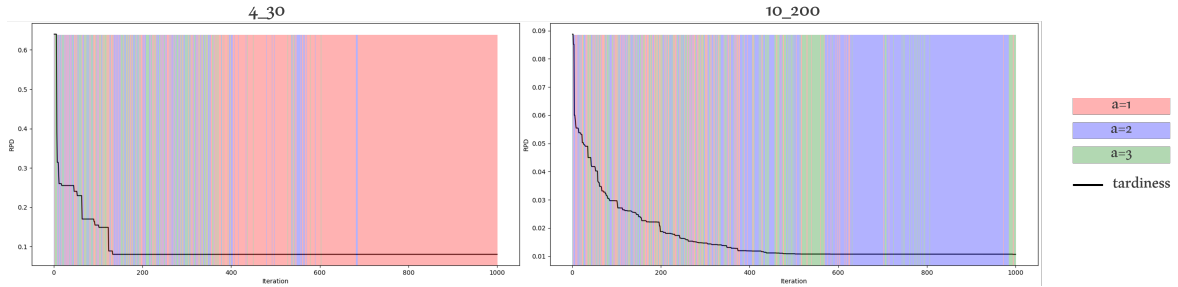


Figure 8: Selection of local search operators at each iteration in the search process for certain instances

them the most influential parameters. Other parameters show weaker and less consistent correlations. To further investigate, we vary each parameter across its range while keeping others at optimal values, observing the changes in three objectives. The results, shown in Figure B.12 with tuned values marked in Table 7, reveal that the Q-ALNS is sensitive to parameter levels, which impact each objective differently. Lower ϵ values significantly reduce tardiness and makespan but increase distance. In contrast, t shows a fluctuating impact on tardiness and distance, with a smaller effect on makespan. This highlights the importance of effective parameter tuning, as applied in Section 5.3.

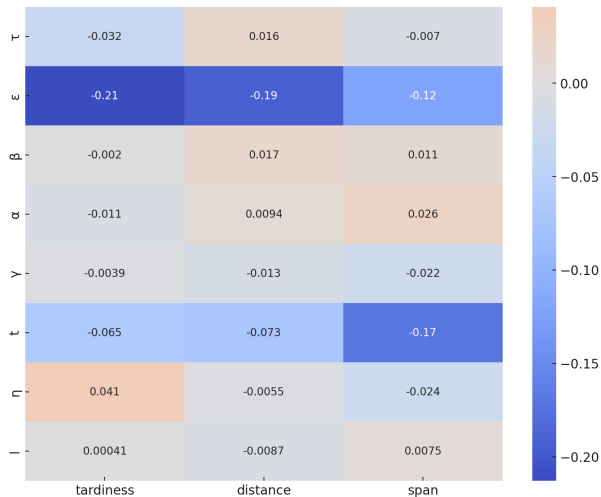


Figure 9: Correlation heatmap between parameters and objective functions

Action set size

The action space in our algorithm is determined by the number of local search operators. After selecting the better-performing local search operators, the Q-ALNS has an action set size of three. We compare this with a larger action space of 16 local search operators (before filtering, as detailed in Section 6.1) to analyze the effect of action space size on the algorithm’s performance. Table 14 presents the results based on three metrics. The AvS values show that the Q-ALNS with a smaller action space (3-action) generally achieves better solution quality, with a lower median AvS than the 16-action space, indicating more consistent performance. The BS metric, representing the RPD of the best solution found, is also better for the 3-action space configuration, suggesting that a smaller, more focused action space leads to more optimal solutions. Interestingly, the 16-action space configuration requires less CPU time on average compared to the 3-action space. This may be due to the larger action space allowing for more diverse and potentially faster exploration paths, while the smaller action space, although producing higher quality solutions, may require more local search steps, increasing computation time.

These findings highlight the trade-off between action space size and algorithm performance. A well-balanced action space is crucial for maintaining a good balance between exploration and exploitation. While a smaller action space with better-performing local search operators can improve solution quality, it may increase com-

putational effort. Conversely, a larger action space can reduce computation time but may lead to less optimal solutions.

Table 14: Comparison of Q-ALNS with Different Action Spaces

Instance		Q-ALNS with 16-action space			Q-ALNS with 3-action space		
Dock	Truck	AvS	BS	T(s)	AvS	BS	T(s)
3	20	0.127	0.017	17.3	0.256	0.008	28.7
4	30	0.231	0.134	34.7	0.179	0.080	40.4
5	50	0.139	0.061	76.4	0.065	0.023	118.9
6	60	0.141	0.117	98.5	0.075	0.029	154.1
7	70	0.574	0.330	162.7	0.367	0.106	216.4
8	100	0.063	0.038	376.1	0.030	0.012	412.2
8	130	0.053	0.037	566.0	0.030	0.016	702.2
9	160	0.023	0.015	953.4	0.015	0.003	1128.4
9	180	0.034	0.023	1288.3	0.015	0.006	1401.4
10	200	0.025	0.020	1645.2	0.014	0.006	1973.5
Average		0.141	0.079	521.9	0.105	0.029	617.6

Reward function

This section analyzes the impact of the reward mechanism on the performance of the Q-ALNS. We compare the original 0-1 reward mechanism with the proposed value-based reward mechanism (detailed in Section 4.2) to understand how different reward structures affect the algorithm’s performance. The results in Table 15 reveal that the value-based reward mechanism achieves slightly better solution quality compared to the original 0-1 reward mechanism, with a lower median AvS indicating more consistent performance. The BS metric, representing the best solution found, is also better for the value-based reward mechanism, suggesting that this reward structure leads to more optimal solutions. Additionally, the value-based reward mechanism requires significantly less CPU time on average, likely due to its more efficient guidance of the search process, which reduces the overall computation time needed to find high-quality solutions.

These findings highlight the effectiveness of the value-based reward mechanism in improving both solution quality and computational efficiency. While the original 0-1 reward mechanism achieves acceptable performance, the value-based reward mechanism offers a better balance between solution quality and computational effort.

Table 15: Comparison of Q-ALNS with 0-1 Reward Mechanisms

Instance		Original 0-1 reward mechanism			Value-based reward mechanism		
Dock	Truck	AvS	BS	T(s)	AvS	BS	T(s)
3	20	0.258	0.025	26.8	0.256	0.008	28.7
4	30	0.062	0.062	76.6	0.179	0.080	40.4
5	50	0.092	0.064	175.5	0.065	0.023	118.9
6	60	0.093	0.040	238.9	0.075	0.029	154.1
7	70	0.477	0.388	285.1	0.367	0.106	216.4
8	100	0.031	0.006	743.9	0.030	0.012	412.2
8	130	0.033	0.021	1172.2	0.030	0.016	702.2
9	160	0.019	0.014	1857.7	0.015	0.003	1128.4
9	180	0.020	0.011	2478.3	0.015	0.006	1401.4
10	200	0.016	0.009	3085.4	0.014	0.006	1973.5
Average		0.110	0.064	1014.0	0.105	0.029	617.6

6.3. Phase 3: Comparison of dock mode decision with pre-set scenarios

In this phase, we compare the Adaptive, Fix, and Mix dock operation strategies. Figure 10 shows boxplots of the three strategies across three objective functions, based on comparisons from 10 instances. To facilitate comparison, the objective function values are normalized using min-max scaling. Our Adaptive strategy performs better in tardiness and makespan. Specifically, the Adaptive strategies achieve an average reduction of 2.2% and 11.7% in tardiness and 5.8% and 0.3% in makespan compared to the Fix and Mix strategies, respectively. However, this may come at the cost of a relatively higher distance, with increases of 4.2% and 1.3%,

respectively. In the fixed dock mode, the alternating arrangement of loading and unloading docks can create geometric symmetry, thereby minimizing the average distance between storage locations and docks. Conversely, in dock modes with indeterminate or fully mixed usage, scheduling tends to prioritize timely allocation, increasing the complexity of transportation paths. Additionally, the fully mixed mode does not achieve better tardiness, likely due to the truck arrival and departure structure. Our Adaptive strategy demonstrates better adaptability to this structure.

Subsequently, we discuss dock utilization under different strategies. The utilization for a given dock i is calculated as the ratio of the actual usage time to the total time period. The utilization U_i of dock i is determined by eq. (43), where n_i is the total number of tasks processed on dock i , $t_{\text{start},j}$ and $t_{\text{end},j}$ are the start and end times of task j , and T_{max} is the maximum end time of all tasks across all docks.

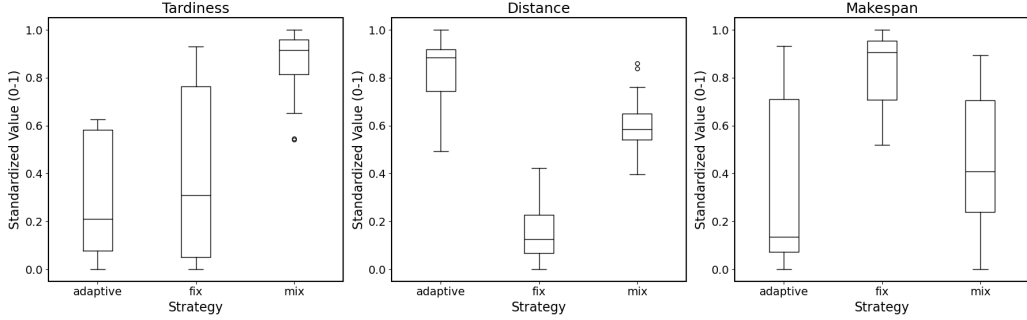


Figure 10: Boxplot of the Adaptive, Fix, and Mix strategies based on tardiness, distance, and makespan

$$U_i = \frac{\sum_{j=1}^{n_i} (t_{\text{end},j} - t_{\text{start},j})}{T_{\text{max}}} \quad (43)$$

Figure 11 shows the Gantt charts for each strategy in a randomly selected instance, where black boxes represent unloading trucks, and white boxes represent loading trucks. The MSM dock significantly improves dock utilization. The Mix strategy consistently maintains high utilization but increases scheduling complexity. The Adaptive strategy, with an average utilization of 89.97%, outperforms the Fix strategy, which has an average utilization of 75.82%. Furthermore, the Adaptive strategy achieves this high utilization with only 37.5% of docks being mixed-use, comparable to the 100% mixed docks in the Mix strategy. This result indicates that the Adaptive strategy achieves similar high utilization with less operational complexity, aligning with the findings of Rijal et al. (2019).

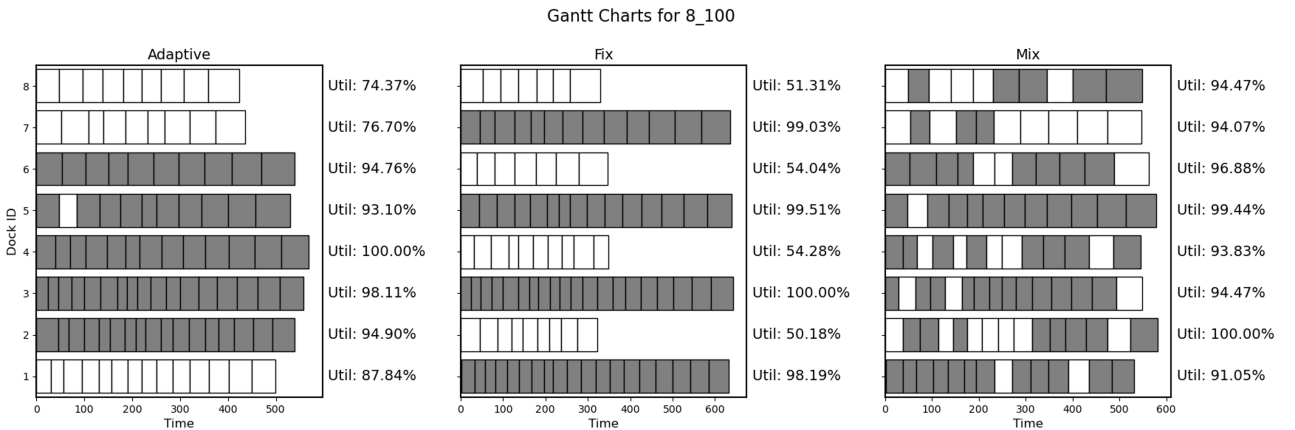


Figure 11: Gantt charts of the Adaptive, Fix, and Mix strategy for the instance 8_200

7. Conclusion

This paper investigates the integrated truck assignment and scheduling problem with dock mode decision, extending the flexibility of mixed service mode docks compared to the commonly used pre-set dock mode strategies in existing research. We constructed a mathematical model that integrates truck assignment, scheduling, and dock mode decisions, aiming to minimize tardiness, makespan, and AGV handling distance. To solve this complex combinatorial optimization problem, we proposed a Q-learning-based Adaptive Large Neighborhood Search (Q-ALNS) algorithm in which Q-learning is embedded into ALNS to guide the adaptive operator selection mechanism.

To validate the proposed approach, we conducted a three-phase experiment. These experiments indicate that the performance of the ALNS relies heavily on filtering better-performing operator combinations, which can significantly enhance the algorithm's adaptability to the problem. The Q-ALNS, which incorporates Q-learning, consistently outperforms the original ALNS and other benchmarks in terms of optimality gap and Pareto front quality, with comparable overhead complexity. Especially in large-scale problems, it takes a shorter time to reach the best solution. This validates the competitiveness of the Q-ALNS in balancing exploration and exploitation. The sensitivity analysis revealed that a well-balanced action space and an effective reward mechanism are crucial for optimizing the performance of the Q-ALNS. Additionally, incorporating dock mode decision strategies results in relatively lower objective function values, more balanced and efficient Gantt charts, and higher dock utilization rates, significantly enhancing the operational flexibility and efficiency of the inbound and outbound processes.

Despite the significant benefits achieved, the current model assumes a level of certainty in operational conditions, which might not fully capture the complexities of real-world scenarios. A promising direction for future research is to extend the model to account for uncertainty, enhancing its applicability to more dynamic and complex environments. On the algorithmic side, the integration of Q-learning into the ALNS algorithm has proven effective, and future work could further enhance the intelligence of parameter selection, improving the algorithm's adaptability and performance.

Acknowledgements

Funding: This work was supported by the National Key Research and Development Program of China [grant number 2021YFB1407003]; and the China Scholarship Council [grant number 202307090057].

References

- Berghman, L. and Leus, R. (2015). Practical solutions for a dock assignment problem with trailer transportation. *European Journal of Operational Research*, 246(3):787–799.
- Bodnar, P., de Koster, R., and Azadeh, K. (2017). Scheduling Trucks in a Cross-Dock with Mixed Service Mode Dock Doors. *Transportation Science*, 51(1):112–131. Publisher: INFORMS.
- Boualamia, H., Metrane, A., Hafidi, I., and Mellouli, O. (2023). A New Adaptation Mechanism of the ALNS Algorithm Using Reinforcement Learning. In Aboutabit, N., Lazaar, M., and Hafidi, I., editors, *Advances in Machine Intelligence and Computer Science Applications*, volume 656, pages 3–14. Springer Nature Switzerland, Cham. Series Title: Lecture Notes in Networks and Systems.
- Boysen, N. and Fliedner, M. (2010). Cross dock scheduling: Classification, literature review and research agenda. *Omega*, 38(6):413–422.
- Buijs, P., Vis, I. F., and Carlo, H. J. (2014). Synchronization in cross-docking networks: A research classification and framework. *European Journal of Operational Research*, 239(3):593–608.
- Chowdhury, S., Marufuzzaman, M., Tunc, H., Bian, L., and Bullington, W. (2019). A modified Ant Colony Optimization algorithm to solve a dynamic traveling salesman problem: A case study with drones for wildlife surveillance. *Journal of Computational Design and Engineering*, 6(3):368–386.

- Guimaraes, F. G., Wanner, E. F., and Takahashi, R. H. (2009). A quality metric for multi-objective optimization based on Hierarchical Clustering Techniques. In *2009 IEEE Congress on Evolutionary Computation*, pages 3292–3299, Trondheim, Norway. IEEE.
- Hermel, D., Hashemina, H., Adler, N., and Fry, M. J. (2016). A solution framework for the multi-mode resource-constrained cross-dock scheduling problem. *Omega*, 59:157–170.
- John, S.-N., Darvari, V.-A., Handl, J., and Kalcsics, J. (2023). GRAPH Reinforcement Learning for Operator Selection in the ALNS Metaheuristic. In Dorronsoro, B., Chicano, F., Danoy, G., and Talbi, E.-G., editors, *Optimization and Learning*, volume 1824, pages 200–212. Springer Nature Switzerland, Cham. Series Title: Communications in Computer and Information Science.
- Karimi-Mamaghan, M. (2022). Machine learning at the service of meta-heuristics for solving combinatorial optimization problems: A state-of-the-art. *European Journal of Operational Research*.
- Karimi-Mamaghan, M., Mohammadi, M., Padeloup, B., and Meyer, P. (2023). Learning to select operators in meta-heuristics: An integration of Q-learning into the iterated greedy algorithm for the permutation flowshop scheduling problem. *European Journal of Operational Research*, 304(3):1296–1330.
- Ladier, A.-L. and Alpan, G. (2016). Cross-docking operations: Current research versus industry practice. *Omega*, 62:145–162.
- Neamatian Monemi, R. and Gelareh, S. (2023). Dock assignment and truck scheduling problem; consideration of multiple scenarios with resource allocation constraints. *Computers & Operations Research*, 151:106074.
- Neamatian Monemi, R., Gelareh, S., and Maculan, N. (2023). A machine learning based branch-cut-and-Benders for dock assignment and truck scheduling problem in cross-docks. *Transportation Research Part E: Logistics and Transportation Review*, 178:103263.
- Pisinger, D. and Ropke, S. (2007). A general heuristic for vehicle routing problems. *Computers & Operations Research*, 34(8):2403–2435.
- Pisinger, D. and Ropke, S. (2019). Large Neighborhood Search. In Gendreau, M. and Potvin, J.-Y., editors, *Handbook of Metaheuristics*, volume 272, pages 99–127. Springer International Publishing, Cham. Series Title: International Series in Operations Research & Management Science.
- Rijal, A., Bijvank, M., and de Koster, R. (2019). Integrated scheduling and assignment of trucks at unit-load cross-dock terminals with mixed service mode dock doors. *European Journal of Operational Research*, 278(3):752–771.
- Ropke, S. and Pisinger, D. (2006). An Adaptive Large Neighborhood Search Heuristic for the Pickup and Delivery Problem with Time Windows. *Transportation Science*, 40(4):455–472.
- Shakeri, M., Low, M. Y. H., Turner, S. J., and Lee, E. W. (2012). A robust two-phase heuristic algorithm for the truck scheduling problem in a resource-constrained crossdock. *Computers & Operations Research*, 39(11):2564–2577.
- Shaw, P. (1998). Using Constraint Programming and Local Search Methods to Solve Vehicle Routing Problems. In Goos, G., Hartmanis, J., Van Leeuwen, J., Maher, M., and Puget, J.-F., editors, *Principles and Practice of Constraint Programming — CP98*, volume 1520, pages 417–431. Springer Berlin Heidelberg, Berlin, Heidelberg. Series Title: Lecture Notes in Computer Science.
- Stephan, K. and Boysen, N. (2011). Vis-à-vis vs. mixed dock door assignment: A comparison of different cross dock layouts. *Operations Management Research*, 4(3-4):150–163.
- Tan, K., Lee, T., and Khor, E. (2001). Evolutionary algorithms for multi-objective optimization: performance assessments and comparisons. In *Proceedings of the 2001 Congress on Evolutionary Computation (IEEE Cat. No.01TH8546)*, volume 2, pages 979–986, Seoul, South Korea. IEEE.
- Turkeš, R., Sörensen, K., and Hvattum, L. M. (2021). Meta-analysis of metaheuristics: Quantifying the effect of adaptiveness in adaptive large neighborhood search. *European Journal of Operational Research*, 292(2):423–442.
- Voigt, S. (2024). A review and ranking of operators in adaptive large neighborhood search for vehicle routing problems. *European Journal of Operational Research*, page S0377221724003928.

- Wilcoxon, F. (1992). Individual Comparisons by Ranking Methods. In *Breakthroughs in Statistics: Methodology and distribution*, pages 196–202. Springer, New York, NY.
- Windras Mara, S. T., Norcahyo, R., Jodiawan, P., Lusiantoro, L., and Rifai, A. P. (2022). A survey of adaptive large neighborhood search algorithms and applications. *Computers & Operations Research*, 146:105903.
- Wolff, P., Emde, S., and Pfohl, H.-C. (2021). Internal resource requirements: The better performance metric for truck scheduling? *Omega*, 103:102431.
- Zhang, Y., Atasoy, B., and Negenborn, R. R. (2022). Dynamic synchromodal transport planning under uncertainty: A reinforcement learning approach. *Transportation Research Record: Journal of the Transportation Research Board*, 2676(3):71–87.
- Zitzler, E. and Thiele, L. (1999). Multiobjective evolutionary algorithms: a comparative case study and the strength Pareto approach. *IEEE Transactions on Evolutionary Computation*, 3(4):257–271.

Appendix A. Detailed Descriptions and Sources of Local Search Operators

The local search operators in ALNS are formed by a combination of destroy, repair, and comprehensive operators. Some operators were adapted from the design ideas in Bodnar et al. (2017), Rijal et al. (2019), but were modified to suit the specifics of our problem.

Our design of destroy operators follows the most commonly used random and greedy operators found in the ALNS literature. The random destruction operator randomly selects a subset of elements from the current solution to remove, creating diversity in the search process. The greedy destruction operator, on the other hand, targets the removal of elements that are likely to lead to immediate improvements in the solution quality when reinserted. The destroy operators in the proposed algorithm are as follows:

- **rRd**: Randomly selecting and removing a truck from all available trucks.
- **rMxTar**: Targeting and removing the truck that causes the most significant delay in the current solution.
- **rMxM**: Targeting and removing the truck with the greatest weighted cargo handling distance from all trucks. The weighted cargo handling distance for each truck is calculated using the formula given in Equation (A.1).

$$\mu_i = \sum_{k \in D} \sum_{s \in S} \sum_{g \in G} x_{ik} h_{is} u_{sg} m_{kg} \quad (\text{A.1})$$

The repair strategies considered in this paper include forward, backward, swapping, and inserting. The repair operators are as follows:

- **iBck**: Swap the removed truck with its preceding truck at the same dock.
- **iFwd**: Swap the removed truck with its succeeding truck at the same dock.
- **iSwap**: Depending on whether it is for unloading or loading, swap the removed truck with another randomly selected unloading or loading truck, not limited to the same dock.
- **iUp**: Reallocate the removed truck to a dock with a higher rank based on handling distance.
- **iDown**: Reallocate the removed truck to a dock with a lower rank based on handling distance.
- **iDockInsert**: Attempt to insert the removed truck at all positions in the truck sequence of the same dock, replacing the current solution if improved.
- **iBtwInsert**: Insert the removed truck randomly in the truck sequence of different docks, replacing the current solution if improved.

The comprehensive operators, distinct from the destroy and repair operators, independently modify an existing solution. The designed comprehensive operators in this paper include the following three types:

- **riInD2D**: Randomly selects two docks used for unloading (D_I) and swaps the trucks they service, while maintaining the sequence of trucks.
- **riOuD2D**: Randomly selects two docks used for loading (D_O) and swaps their serviced trucks, keeping the truck order unchanged.
- **riFlxD2D**: In mixed-mode docks (D_F), randomly selects two docks and swaps their serviced trucks, again preserving the truck sequence.

Appendix B. Sensitive of the Q-ALNS to its parameters

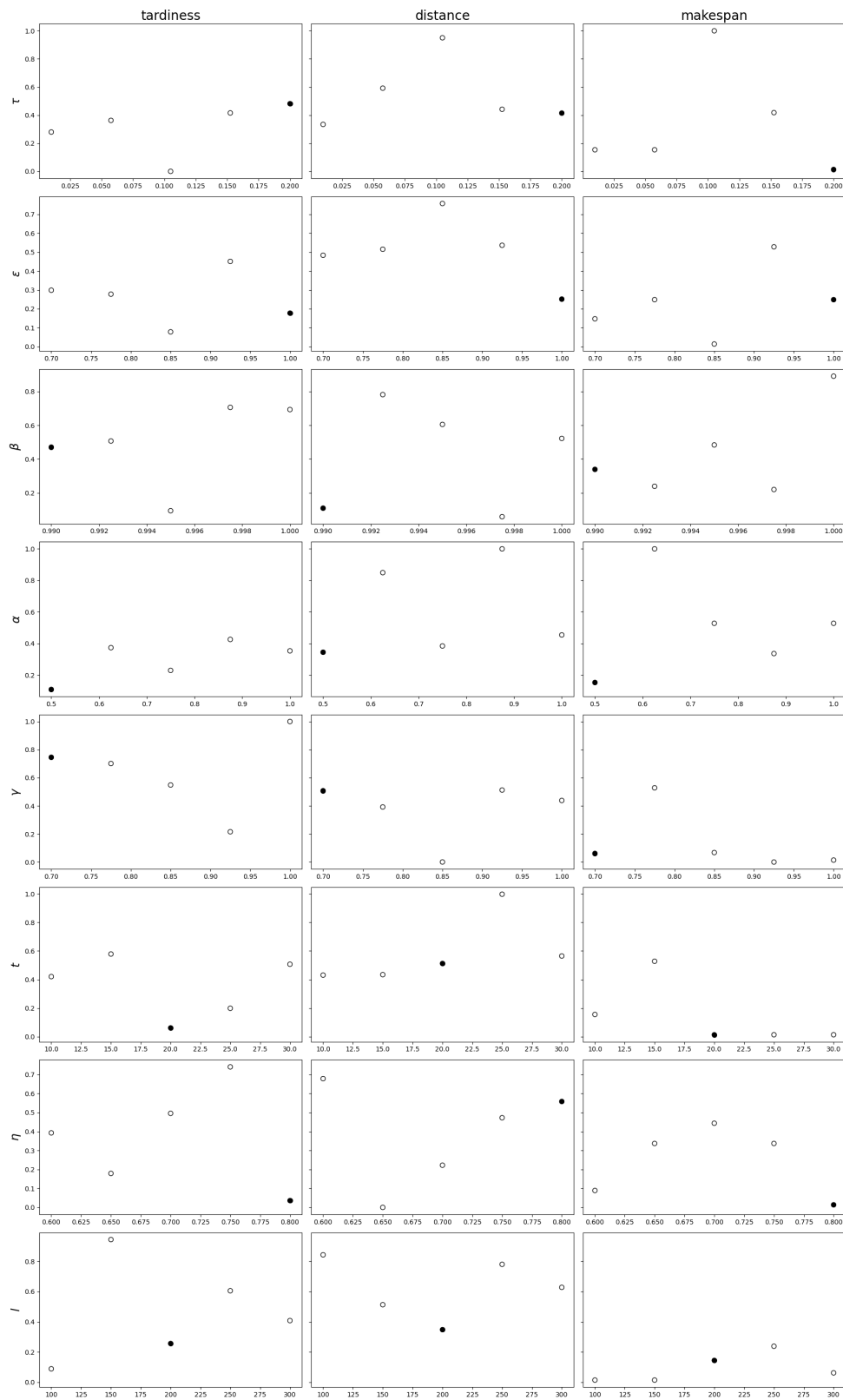


Figure B.12: Sensitive of the Q-ALNS to its parameters based on tardiness, distance, and makespan